

Omran E. Frihy · Moheb M. Iskander  
Abd El Moniem A. Badr

## Effects of shoreline and bedrock irregularities on the morphodynamics of the Alexandria coast littoral cell, Egypt

Received: 4 December 2002 / Accepted: 5 April 2004 / Published online: 18 May 2004  
© Springer-Verlag 2004

**Abstract** Beach-nearshore profiles combined with beach and surficial sediment samples were analyzed in conjunction with wave, current, littoral drift and sea-level data to determine the effect of bedrock on morphodynamic processes within the littoral zone of Alexandria on the Mediterranean coast of Egypt. This 14.5-km-long littoral cell is bounded by pronounced embayments and pocket beaches separated by headlands which prevent bypassing of beach sands, in effect making this cell a large, semi-closed basin. The compartmented nature of this cell acts together with the rough irregularity of the rocky seafloor to trap a thin veneer of sediment (< 3 m thick), showing proportional mixing between two sedimentary provinces. A modern fine-grained sediment facies consisting of mixed carbonate/siliciclastic sand flanks most of the nearshore zone down to a depth of 8–10 m. Beyond this depth, considered to be the depth of closure, a relict late Pleistocene to mid-Holocene coarse-grained facies composed of biogenic carbonate sand is found. Along a short section of the coastline (km 3–6), the coarser sediment also occupies the nearshore zone. Over most of the study area the two sediment types are mixed in various proportions, largest mixing coinciding with poorest sorting. Profile analyses revealed seasonal changes in sediment volume along the coast which closely follow the cyclicity of seasonal changes in wave climate. The present shoreline orientation, headlands and rough, irregular rocky seabed are reflected in the erosion/accretion pattern, sediment characteristics, and the reversibility of longshore currents and littoral drift. Although there is a marked deficiency in the sediment balance, the sand budget for this cell, including artificial material ( $2.339 \times 10^6 \text{ m}^3$ ) has increased slightly by  $0.041 \times 10^6 \text{ m}^3 \text{ year}^{-1}$  as a result of engineering works carried out to widen the coastal road (Corniche). In addition to the physical properties of the bedrock

(degree of induration), the accelerating sea-level rise during the Holocene and human influences, the modern morphology of the coast, the erosional seabed features in the nearshore zone, and the texture of seabed sediments are all controlled by the original geometry of the coast which consisted of an elevated subaerial ridge.

### Introduction

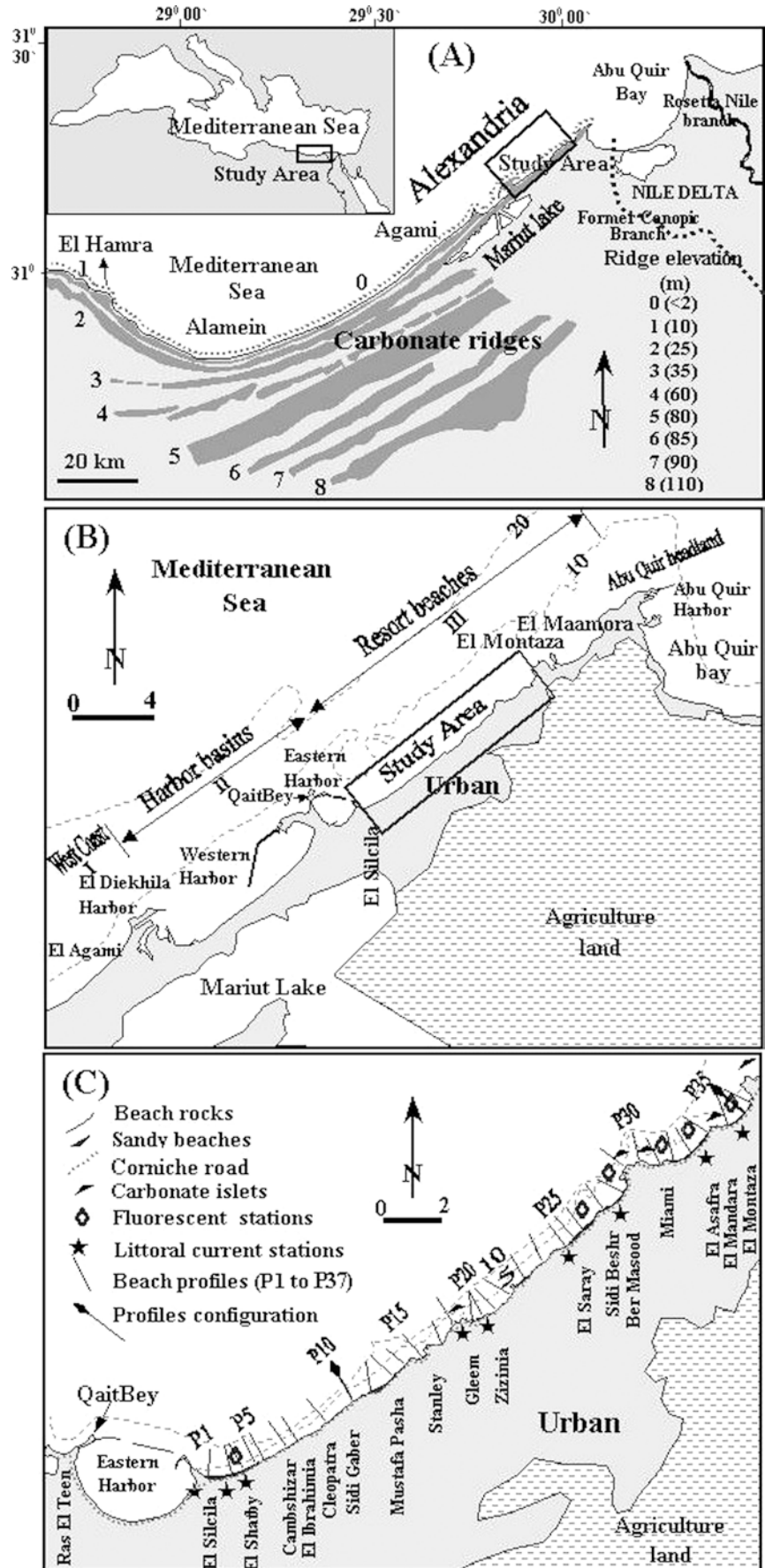
The ancient city of Alexandria is located immediately west of the Nile delta and was founded by Alexander the Great in 332–331 B.C. Geomorphologically, Alexandria is built on a narrow coastal plain consisting of Pleistocene carbonate-sand ridges (Fig. 1A). This coastal plain represents the most eastern part of ridge #2 (Abu Sir), which has been assigned a “main Monasterian” age (Shukri et al. 1956). It is backed to the south by various land-use units including urban areas, Mariut lake, inland depressions, desert, and agricultural land (Shukri et al. 1956; Warne and Stanley 1993).

Alexandria is considered today one of the oldest, continuously existing cities of the world. It is the second largest city in Egypt and one of the major ports in the Mediterranean Sea, besides being an important commercial, business, industrial and cultural center. Furthermore, a number of submerged archeological sites have recently been discovered off the Alexandria coastline, which is also the principal seaside resort of Egypt, attracting about two million visitors every summer. The city hosts four harbors: El Diekhila Harbor, the Western and Eastern harbors and Abu Quir Harbor (Fig. 1B).

Generally, the 100-km-long coastline of Alexandria is oriented SW–NE and is bordered by a highway known as the Corniche. The coastline can be divided into three sectors based on morphological character: resort beaches to the west of Alexandria beginning at El Agami, the Western Harbor basins, and the resort beaches from El Silcila to the Abu Quir headland (Fig. 1B). These sectors are separated by major headlands at El Agami,

O. E. Frihy (✉) · M. M. Iskander · A. E. M. A. Badr  
Coastal Research Institute, 15 El Pharaana Street,  
El Shallalat, 21514 Alexandria, Egypt  
E-mail: Frihyomr@link.net

**Fig. 1A** Map of the western Mediterranean coast of Egypt showing the locations of the Alexandria region and the shore-parallel limestone ridges partially extending across the study area. The limestone ridges are numbered #0 through #8 from north to south (modified after Butzer 1960). **B** Main geomorphological units of the study region. **C** Coastline configuration of the littoral zone of Alexandria comprising beach embayments and pocket beaches separated by rocky headlands. Also shown are the positions of 37 beach-nearshore profile lines examined in this study. Positions of littoral current and littoral drift stations are indicated by symbols. Depth contours in meters



QaitBey, El Silcila, El Montaza and Abu Quir. The coast west of Alexandria is characterized by straight, carbonate-sand beaches of variable width.

The focal point of this study, the coastline between El Silcila and El Montaza, constitutes a major natural asset for the region's summer resort industry (Fig. 1C). This zone is divided into a series of discrete sedimentation sub-cells, with beaches confined between pronounced headlands and embayments ranging between 0.3 and 3.5 km in length (Figs. 1C and 2A). The coast is mostly rocky, comprising low sea cliffs and offshore shoals, with very few beaches fronting the resort facilities constructed along most of the Corniche (Fig. 2C, F). The original beach sands are composed of biogenic carbonate-rich, medium to coarse sands, varying from loose to fairly well-indurated deposits of shell fragments, quartz, heavy minerals and other debris (Hilmy 1951; El Wakeel and El Sayed 1978). Beach and seabed sediments are derived primarily from the adjacent Pleistocene limestone ridges located along the western coast of Alexandria, and the local rocky limestone outcrops forming ridge #2 (Abu Sir; Figs. 1A and 2B). These rocks consist mainly of sandy limestone typical of the Pleistocene ridge formations and beach rocks (El Sayed 1987, 1988). The ridges run parallel to the coast in the backshore and in upland areas from Alexandria to Sallum on the Egyptian/Libyan border (Fig. 1A). They increase progressively in elevation from ~10 m along the coast to ~100 m some 40 km inland (Shukri et al. 1956). The origin of these ridges ranges from marine, such as offshore bars and beach deposits, to eolian (Fourtau 1893; Shukri et al.; 1956; Said et al. 1956; Butzer 1960; Lindell et al. 1991). Most of the Alexandria beaches currently appear to be experiencing active erosion with evidence of sand losses (Fig. 2B), only a few beaches being accretionary or nearly stable (El Wakeel et al. 1980; Iskander 2000).

The purpose of this study is to evaluate coastal processes, seasonal factors and human interventions influencing morphodynamic changes in the littoral zone of Alexandria, in particular the role of beach and bedrock materials in governing the morphology of the beach and littoral zone sediment budget as well as the prevailing driving forces. The petrology of the beach and seabed sediments is determined to assess sedimentary provinces, their implications for delineating the depth of closure, and the possibility of using these for beach nourishment. Based on the morphodynamic nature of the littoral zone and the elevation of the upland area, the vulnerability of the Alexandria waterfront to the predicted rise in sea level is evaluated.

---

### Environmental setting

The Mediterranean Sea around Alexandria shows a typical semi-diurnal microtidal regime. Long-term daily gauge records indicate maximum and minimum astronomical tidal water levels of +33.8 and -15.9 cm, respectively, giving a maximum tidal range of 49.7 cm

(Frihy 1992). Storm surges can raise the sea level by about 40 cm, causing overtopping of the beach and the Corniche (Hamed and El Gindy 1988). Winter storms impact the coast with a frequency of about 14 per year, with wind speeds reaching 35 knots.

---

### Engineering structures

As a consequence of the sediment deficiency in the Alexandria littoral cell, beaches have been protected as early as 1934 to prevent further erosion and to provide new recreational sandy stretches. The Corniche highway, ~20 km from Montaza to the promontory of the Ras El Tin Palace, is protected from the sea by a vertical wall. In addition, 4-t concrete blocks have been emplaced along the coast, beginning in 1984. Breakwaters have been constructed to protect the El Diekhila Harbor, Western Harbor, Eastern Harbor and Abu Quir Harbor. Finally, several artificial beach nourishment projects, some combined with the construction of massive groins, have been out at El Shatby, Stanley, El Asafra, El Mandara and Abu Quir (Fig. 2D). A large amount of sand ( $0.31 \times 10^6 \text{ m}^3$ ) has been imported from the desert some 150 km to the south of Alexandria (Frihy and Dean 1992; Iskander 2000). In general, the nourishment projects have been effective in protecting and improving amenities on the eroding beaches.

More recently, i.e., between 1999 and 2002, two detached breakwaters were constructed in order to reduce coastal erosion at the Cleopatra beach. These were built in the active surf zone at water depths between 3 and 4 m, spaced 110 m apart and extending 120 m parallel to the beach. Two additional breakwaters are expected to be built in the nearshore in the near future.

A large-scale construction project was implemented over five successive phases between March 1998 and March 2002 to widen the Corniche (Fig. 2E, G). The project provides three to five car lanes instead of two in each direction. Associated with this new coastal road is a wide walkway with rest and park areas along the seaward side (Fig. 3). The ultimate purpose of the project is to smoothen road curvatures and upgrade traffic flow to meet demands for city development. The road is now 45 m instead of 28 m wide over a distance of 14.5 km between El Montaza and El Silcila (Fig. 2E). The cross section in Fig. 3 shows the sand-fill material under the widened part of the road, which is separated from the sea by a buffer zone comprising ~300–800 kg of graded dolomitic quarry stone boulders supported by a vertical concrete wall. A thin layer of geo-textile, lined by a gravel filter, is emplaced between the sand-fill and buffer zones to mitigate possible winnowing of the fine sediment by wave-induced currents and to reduce hydrostatic pressure (Fig. 2G). A series of 10-t concrete blocks, extending 20 m seaward, have been placed to protect both the vertical concrete wall and the dolomitic limestone boulders from the sea (Fig. 3).

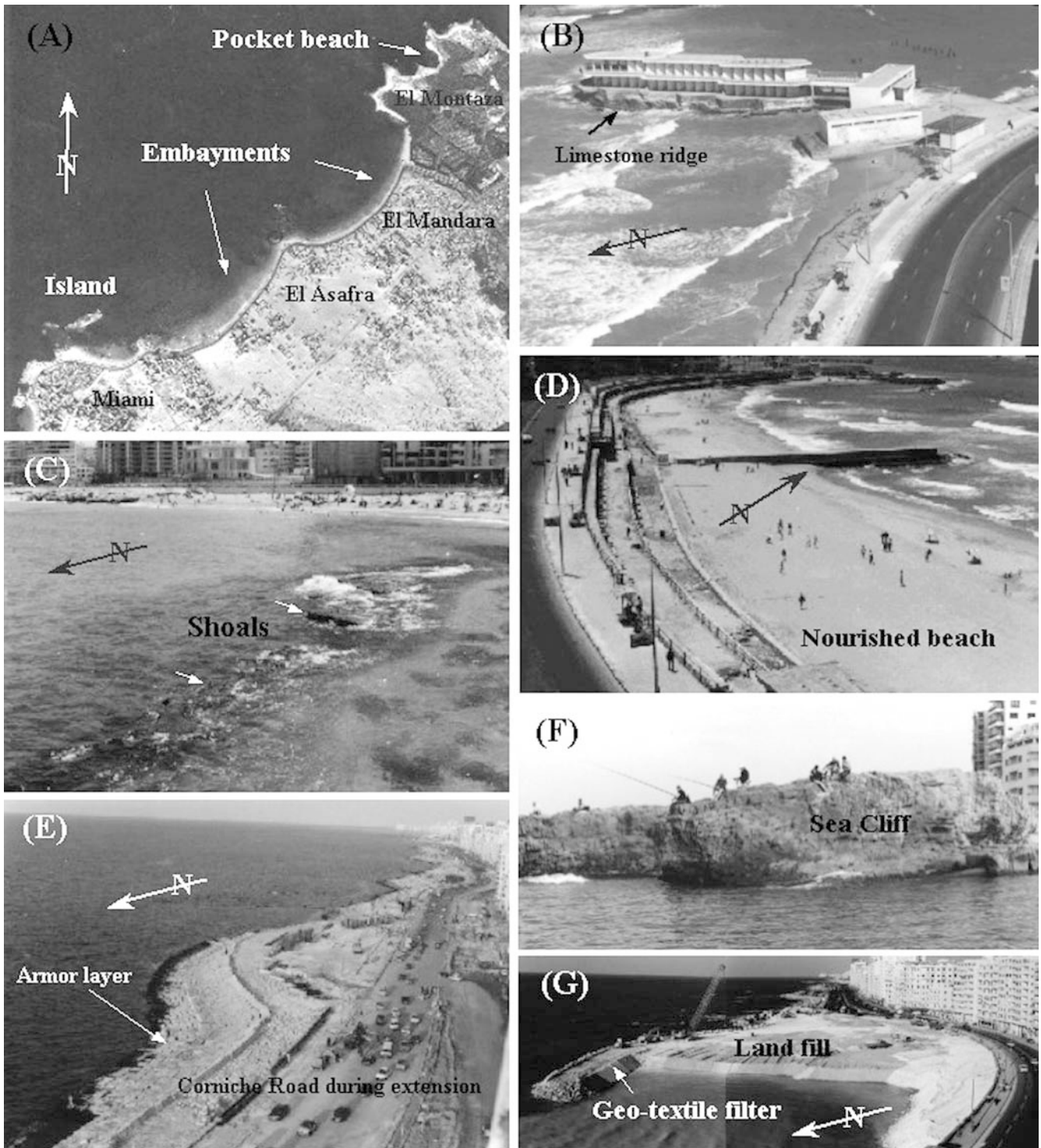
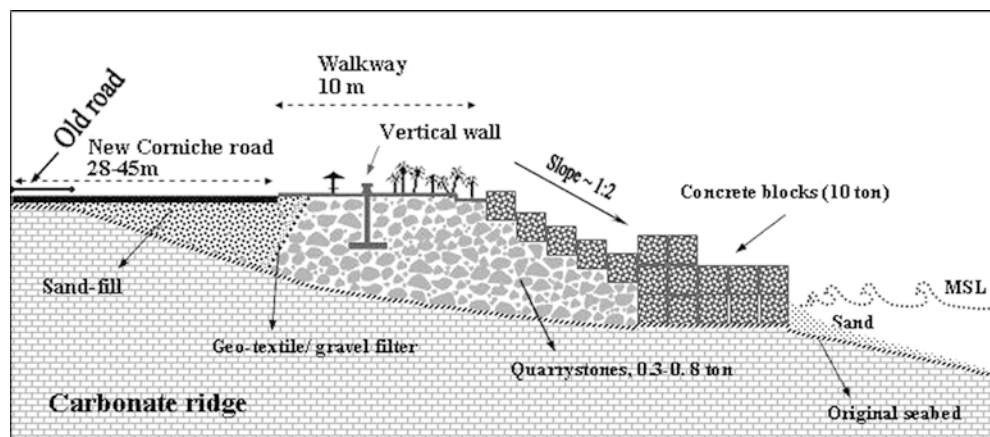


**Fig. 2A–G** Photographs of the Alexandria coast showing **A** nearshore islets fronting an undulating coastline of large embayments and pocket beaches (aerial photo 1955), **B** a casino built on a limestone remnant ridge showing signs of erosion, **C** a limestone ridge forming submerged shoals, **D** the nourished beach at El Asafra in 1988, **E** the status of the widening project of the coastal road (Corniche) in July 2001, **F** the sea cliff backing the coastline, and **G** the final phase of the extension of the Corniche and protective works in February 2002

### Materials and methods

A monitoring program spanning the study area between El Silcila and El Montaza was undertaken over a 24-month period, from October 1998 through October 2000. The locations of the monitoring sites and field activities are indicated in Fig. 1C. A total of 37 beach-nearshore profiles (up to 10-m water depth) were

**Fig. 3** Cross-shore section of the Corniche road extension project in Alexandria, showing the main project components



surveyed twice yearly. A depth of 10 m was chosen to represent the seaward limit of the active littoral zone, corresponding to the closure depth at a maximum distance of  $\sim 1$  km offshore. The profiles extend from a baseline fixed along the Corniche, with an orientation profile approximately perpendicular to the coastline (Fig. 1C). The distance between the profiles ranged between 125 and 610 m. The elevation of the Corniche, backing the beach, was also measured to evaluate its vulnerability to future sea-level rise (SLR). The road and beach leveling as well as depth soundings were adjusted to mean sea level (MSL) using local, fixed benchmarks of known elevation. Seaward of each profile, soundings were taken every 10 m from the baseline up to a distance of 250 m to locate the seabed within the nearshore zone, and then at 50-m intervals up to the 10-m depth contour. Field surveys were carried out during fair weather twice a year, using a rubber boat equipped with a GPS and echo-sounder to determine seasonal variability in seabed elevation and sediment volume changes. Survey periods were in the autumn (September/October) and spring (April/May).

A total of 139 bottom samples were collected every 100 m along the surveyed profile lines during the first survey period in October 1998. In addition, 49 beach samples were obtained from the upper few centimeters by pushing a plastic sample jar into the surface of the sand, whereas bottom samples were collected by means of a grab sampler (Fig. 1C).

In the laboratory, grain-size analyses were carried out by standard ro-tap sieving using one-phi sieve intervals. The phi scale notation of Krumbein (1963), where  $\phi$  equals the negative logarithm to the base two of particle diameter in millimeters, was used as a size scale. The mean grain size ( $Mz$ ) and standard deviation ( $\sigma_1$ ) for each sample was calculated using the formulae of Folk and Ward (1957). The resulting values of  $Mz$  in phi units were converted into millimeters according to the transformation  $(mm) = 1/2^\phi$ . Carbonate contents were determined using a calcimeter for 165 representative samples. The interpolation of  $Mz$ ,  $\sigma_1$ , carbonate content and depth contours was accomplished by means of the Surfer

software, applying the linear interpolation method to provide areal distribution.

In addition, 14 samples were selected for petrologic analysis of the sand fractions, seven for each of the fine- and coarse-grained end members. Relative percentages of four sand-sized components were calculated from point counts of  $> 400$  grains per sample (method according to Frihy and Stanley 1988). A number of mineralogical (light, heavy minerals and carbonate particles) and faunal (Foraminifera, ostracods, gastropods, pelecypods, bryozoans and echinoids) components were identified. Light minerals mainly comprise quartz and feldspar. Carbonate particles consist of grains, pellets and oolites. Common molluscan fauna were identified in selected samples. Percentages of the total relict (iron-stained) grain components were calculated relative to the total grain counts in each sample.

Daily longshore current speeds and directions were measured at nine stations along the coast (Fig. 1C). Longshore current measurements were obtained inside the surfzone at water depths ranging from 1.2 to 1.5 m by tracking the movement of a buoy, and measuring the time it took to travel a distance of 20 m in the longshore direction. Measurements of current speed and direction were taken twice a day, once in the morning and again in the afternoon. Littoral drift was also determined at six stations by observing the dispersal of fluorescent tracer sands (Fig. 1C), using the field and laboratory approach of Ingle (1966).

Wave data were analyzed based on records measured at El Hamra pier, located 120 km west of Alexandria (Fig. 1A). A pressure wave gauge (Inter Ocean System S4DW) was installed in approximately 7-m water depth off the pier. The gauge recorded wave and current spectra for 20 min every 4 h. In the laboratory, data were transferred to a PC for analysis. Wave data were compiled for a composite 10-month period including the months of January, August, September, October, November and December in 1998, and January, February, April and May in 1999. In the intervening months the wave gauge system failed to provide useful data. The wave data were first back-refracted to deep water, and

then ray-traced shoreward to the local region, applying the nonparallel depth contour technique of Silvester and John (1993). In order to compensate for the nonparallel nature of contours, the term  $\sin\alpha$  in Snells law was replaced by  $\sin\alpha^*$ , where  $\alpha^*$  represents the angle between the local wave angle and the local contour at each point.

Waves are responsible for driving the nearshore current system which, in turn, is responsible for longshore sediment transport. When waves approach the coast at an angle, they cause sediment to be transported along the shore. The direction and magnitude of the longshore current and littoral drift depend on the effective angle of the incident waves and the average shoreline orientation. The modified N-line model of Perlin and Dean (1983) was applied to determine wave directions (exposures) inducing longshore transport along the coastline of the study area. Results obtained enabled us to diagrammatically determine the wave angle which would change the net longshore sediment transport direction from the NE or from the SW. In addition, in defining wave exposure, we identified those components in the wave rose of Alexandria which were able to induce longshore transport on both sides of the shore-normal line. More details are given in Perlin and Dean (1983) and, for the study region, in Iskander et al. (2004).

## Results

Along wave-dominated coasts such as in Alexandria, the main coastal processes controlling modifications in the littoral cell are waves, currents and littoral drift. These processes are interrelated with the petrologic characteristics of beach and seabed sediments, carbonate contents, the orientation of the shoreline, bedrock morphology, and seasonal changes in sediment volume. The sediment basically consists of two hydraulic populations, a fine-grained one and a coarse-grained one, each occupying a specific zone. Where the two zones overlap, the two populations are mixed in various proportions reflected in their textural characteristics.

The statistical relationships, the spatial distribution patterns of grain-size parameters (mean grain size and grain sorting), and the carbonate contents of beach and seabed sediments are used in this study to interpret sedimentary provinces and morphodynamics.

### Petrology and carbonate content

Petrologic analyses of representative sediment samples indicate that both the coarse- and fine-grained sediments display some marked differences in their mineralogic and faunal contents (Fig. 4A). Moreover, grains of the coarse-grained sediment population tend to be more rounded than those of the fine-grained one. Both the faunal and terrestrial petrologic components of the coarse-grained sediments are iron-stained, yellow and reddish-orange to brown (oxidized), and markedly

**Fig. 4A** Relative percentages of major terrestrial and biogenic components in representative samples in the fine- and coarse-grained sands. **B** P10 and P35 are examples of the beach profile configuration characterizing the study area. **C** Positions of sediment samples. **D** Mean grain-size distribution of beach and surficial sediments. The boundary between the recent fine- and relict coarse-grained sands positioned the closure approximately between 8 and 10 m. **E** Distribution of standard deviation (sorting) values. **F** Distribution of carbonate contents. Bathymetry of October 1998 is superimposed (depth contours in meters). Profile locations are given in Fig. 1C

corroded (>99% of the counted grains). The fine-grained sediment components are mostly unstained (<1% of particles), consisting of yellowish gray, white to tan carbonate and quartz particles. The sand of the coarse-grained group reaches the highest average carbonate content (73%) but ranges from about 0 to 100%. The fine-grained sands (Fig. 4A), by contrast, have an average carbonate content of 43% and range from 25 to almost 100%. Shells are more frequent in the coarse-grained sediment (15%) and occur mostly as fragments, as compared to the fine-grained sand which mostly comprises whole tests (8%). Quartz and heavy minerals are the main accessory terrestrial components in the examined sediment groups. The coarse-grained sands are characterized by relatively low proportions of quartz (12%) in comparison to the fine-grained ones (44%). The relative percentages of heavy minerals are higher in the fine-grained sediment group (6%) and very low in the coarse-grained one (0.9%).

To interpret relict fossils, the following shallow marine faunas were identified: *Glycymeris insubricus*, *Donax semistriatus*, *Donax trunculus*, *Donax venustus*, *Chamelea gallina*, *Gibbula umbilicaris*, *Turbonella doli-um*, *Bittium exiguum*, *Hinia pygmaea*, *Turritella* sp., *Modiolus auriculatus*, *Brachiodontes variabilis* and echi-noid spines.

The spatial distribution of mean grain sizes, grain sorting and carbonate contents across the study area reveals diverse but distinct spatial patterns (Fig. 4D–F). In general, the mean grain size of the sediment increases in a seaward direction. An exception is observed between km 3 and 6, where relatively coarse sands are also found on the beach and in the nearshore zone. Having identified two sediment groups, it is possible to interpret, at least in a general way, their spatial distributions across the littoral cell of Alexandria. The fine-grained sediment group (fine and medium sand; 0.15–0.45 mm) mostly covers the nearshore zone whereas the coarse-grained sediments (medium and coarse sand; >0.45–1.0 mm) occur mostly further offshore beyond the 8–10 m depth contour (Fig. 4D). The spatial distribution of sorting indices across the study area demonstrates a general seaward decrease in standard deviation, i.e., a tendency toward better sorting with increasing water depth (Fig. 4E). Spatially, both fine- and coarse-grained sediments are distributed sub-parallel to near-shore topographic features and contours, defining west-to east-trending belts (Fig. 4D–F). In the alongshore

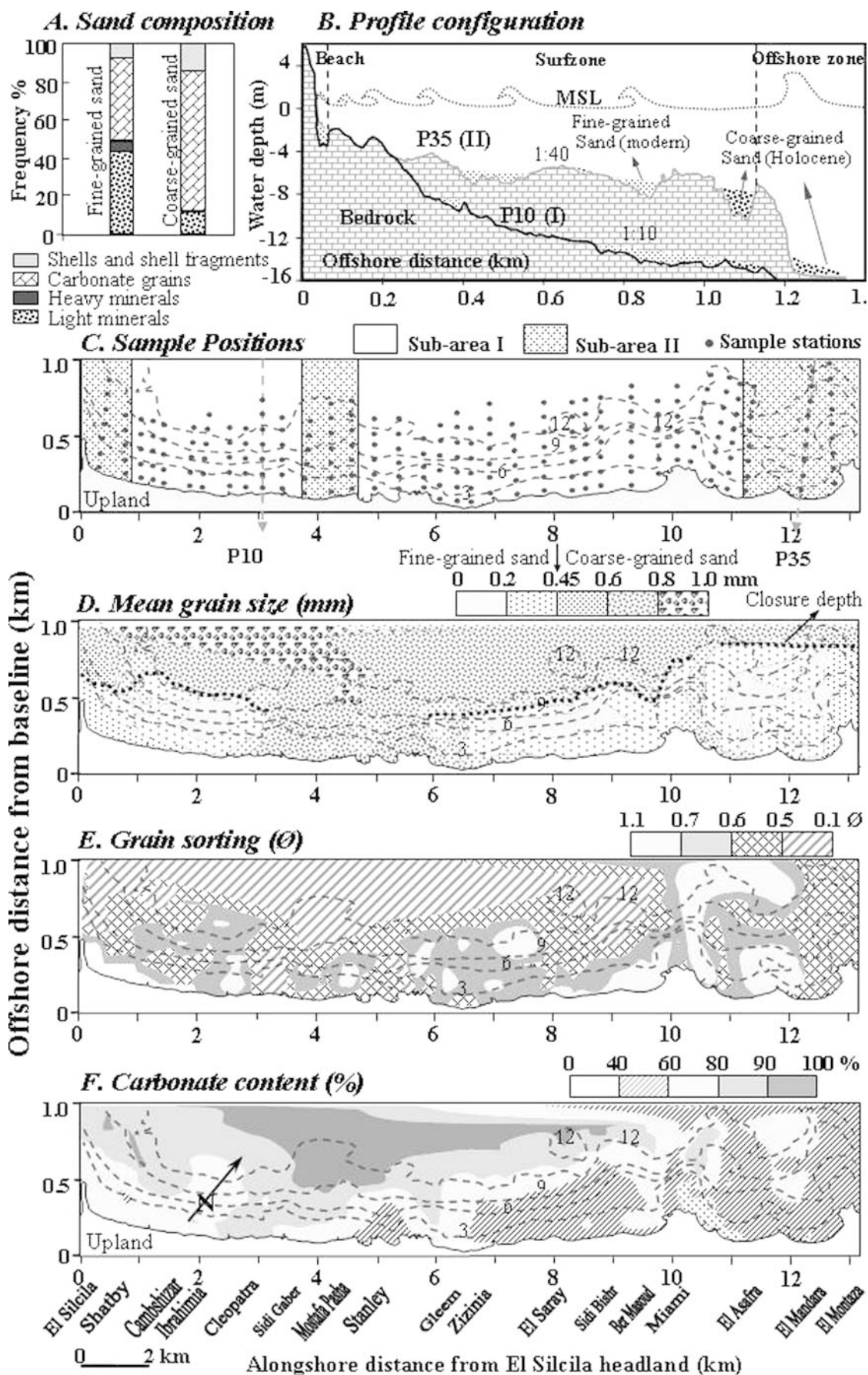
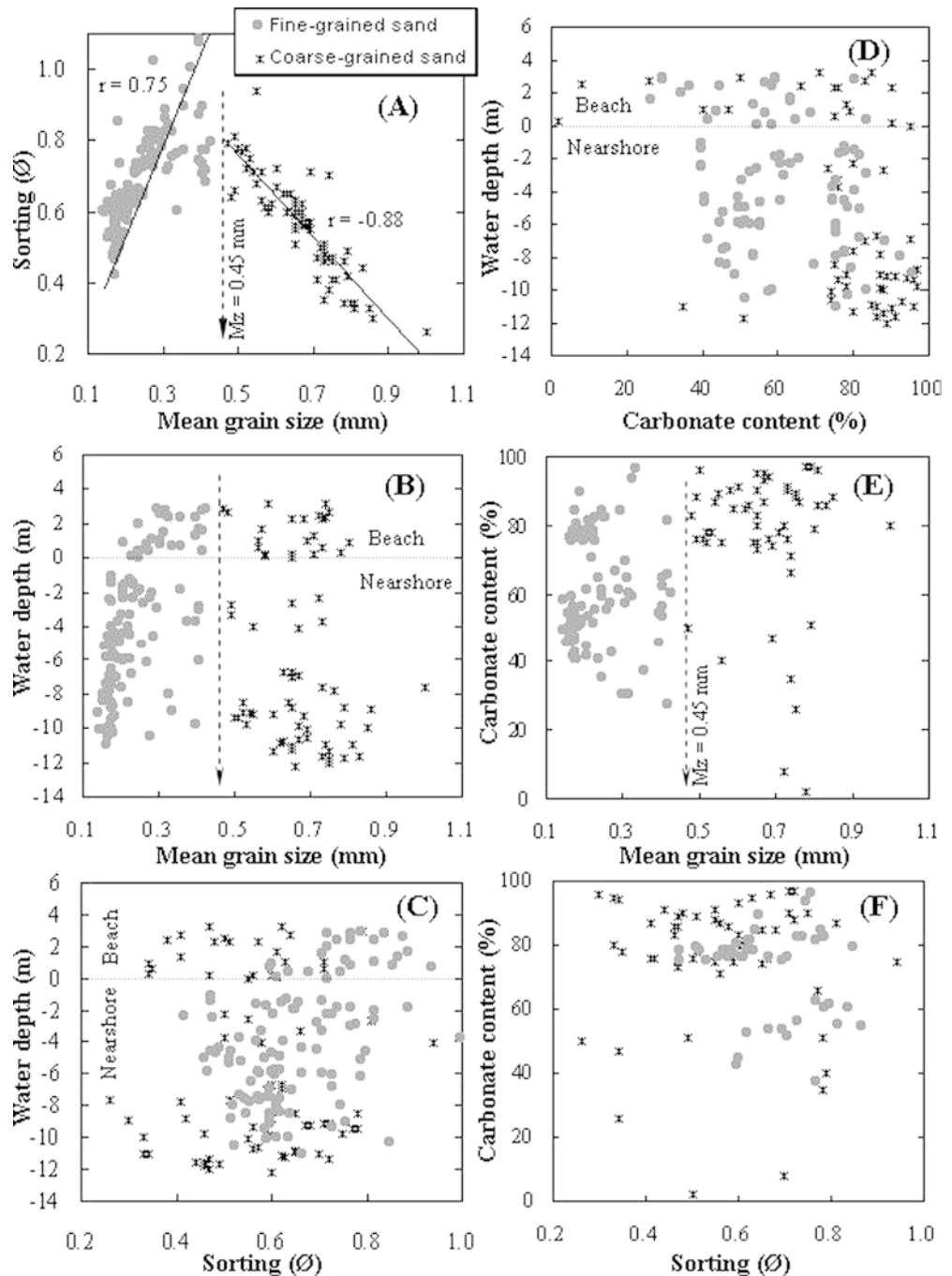


**Fig. 5A–F** Scatter plots of fine- and coarse-grained sediment group samples (188 samples). **A** Sorting versus mean grain size. **B** Water depth versus mean grain size. **C** Water depth versus sorting. **D** Water depth versus carbonate content. **E** Carbonate content versus mean grain size. **F** Carbonate content versus sorting ( $r$  correlation coefficient)



direction, carbonate contents are generally higher in the western part (80–90%) than in the eastern part (<60%) of the study area and by and large increase in an offshore direction (Fig. 4F).

#### Textural relationships

Since it is difficult to interrelate various textural parameters on the basis of their spatial distribution patterns alone, the interpretation has been supplemented by bivariate diagrams between mean grain size, sorting, carbonate contents and water depth (Fig. 5). The data

show that a mean grain size of 0.45 mm clearly delimits two groups of data points, corresponding to a fine- and a coarse-grained sand population. The latter includes <3% granules (2–4 mm). The two populations are indicated by different symbols in the various plots of Fig. 5. The upward-converging trend lines described by the data points in the diagram of mean grain size versus sorting (Fig. 5A) suggest that the two parameters are controlled by progressive mixing between the two sand populations, the coarse end member being better sorted than the fine end member. Thus, the mean grain sizes of the fine-grained group vary in the range 0.15–0.43 mm (average = 0.24 mm) whereas sorting values are 0.42–1.08  $\phi$



(average = 0.67  $\phi$ ). In the case of the coarse-grained population, mean grain sizes are 0.47–1.0 mm (average = 0.67 mm) whereas sorting values are 0.26–0.94  $\phi$  (average = 0.56  $\phi$ ). Due to the mixing process, the two parameters are positively correlated in the fine-grained population ( $r = 0.75$ , 99% level of significance) whereas they are negatively correlated in the coarse-grained population ( $r = -0.88$ , 99% level of significance). At a mean grain size of 0.45 mm, the two populations have their poorest sorting, indicating equal mixing.

The mean grain size and sorting of the two sediment groups were also plotted separately against water depth (Fig. 5B, C) and carbonate content (Fig. 5D–F). Although no statistically significant correlations were observed, the plots nevertheless reveal important spatial relationships between the parameters. Thus, the plot of mean grain size versus water depth (Fig. 5B) shows that both populations occur from the beach out to the offshore limit of sampling at  $\sim 12$  m of water depth. From Fig. 5D we know that the two populations are spatially well separated, both alongshore and offshore. The same applies to carbonate content, mean grain size, and water depth (Fig. 5D, E). As would be expected, no clear relationship was observed between sorting and water depth (Fig. 5C) or carbonate content (Fig. 5F), suggesting that mixing between the populations occurs over the whole study area.

#### Seafloor configuration

The bathymetric data reveal considerable longshore and cross-shore variability in seabed morphology and slope. A visual examination of the bathymetric profiles allows the discrimination of two main groups, each characterizing a particular subsection of the study site. Profiles P10 and P35 are taken as representative examples for each group (cf. Fig. 1C for location). The two sub-zones are characterized by profiles displaying highly irregular bedrock of diverse slopes (Fig. 4B, C). In general, the profiles of sub-area I have relatively steeper surfzone seabed slopes (1:10) compared to those of sub-area II (1:40). The first profile group represents a sub-zone located in the sector from El Shatby-Mostafa Pasha to Stanley-Miami, whereas the second group represents a sub-zone extending from El Silcila-El Shatby, Mostafa Pasha-Stanley, to Miami-Montaza (Fig. 4C). Sub-zone II is partially covered by a thin veneer of mostly artificial beach sand from the surf zone down to a water depth of 4 m (Fig. 4B), whereas bedrock is partially exposed in the offshore. Exposed bedrock is scattered throughout the study area but is more dominant in the offshore at water depths between 5 and 10 m. Seabed without sand cover constitutes >20 and 50% at the depth zones 0–5 and 5–10 m, respectively. The longshore distribution of exposed offshore bedrock is closely related to the position of coastal limestone ridge #0 (Fig. 1A). These bedrock outcrops form the most pronounced morphological feature of the entire Alexandria

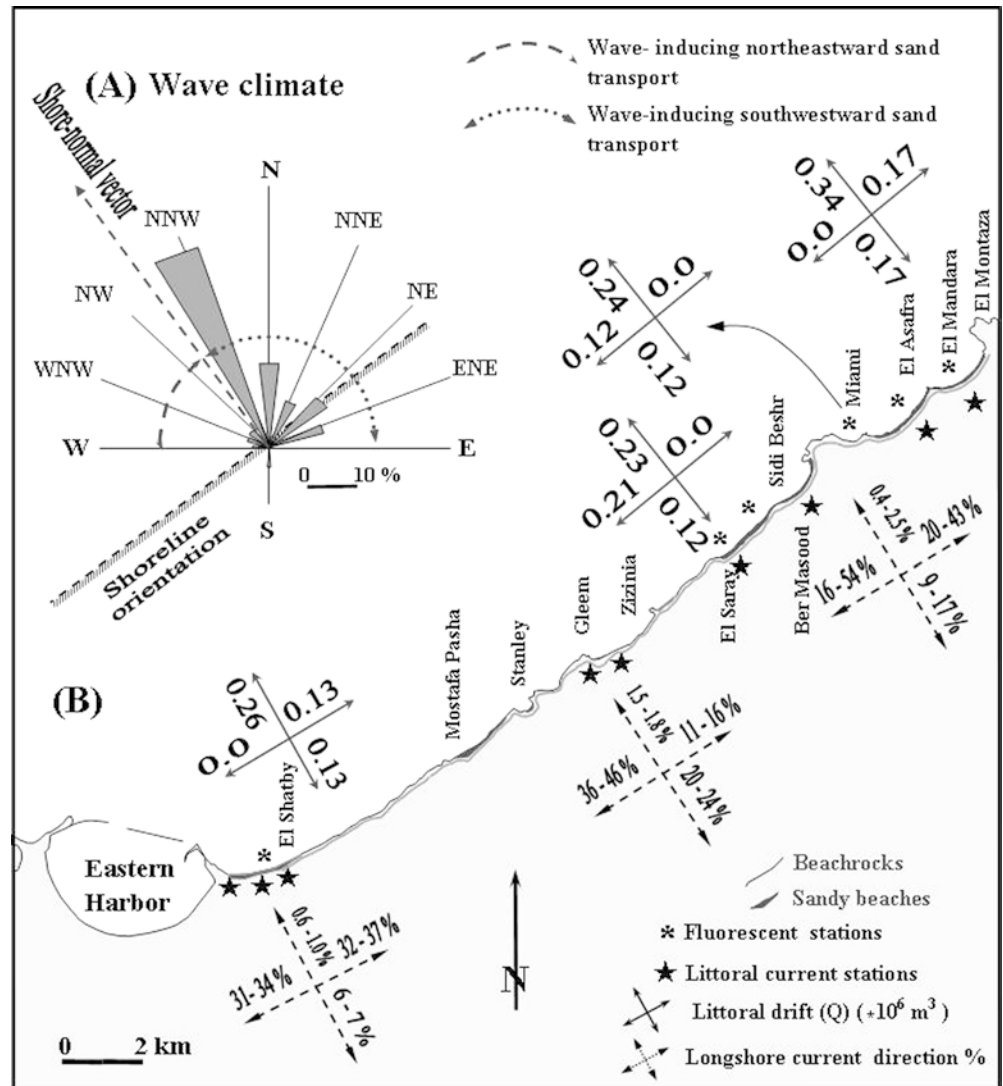
littoral cell. Parts of these outcrops extend above the mean water level to form a series of shore-parallel islets fronting the coastline at an offshore distance of approximately 300 m (Fig. 2A). Remnants of these outcrops form bottom shoals as well as parts of the beach rock along the Alexandria coast. In some cases the beach rock covers rocky limestone headlands isolating individual embayments along the shore. The beach rock is mostly composed of marine shells (mollusks, coralline algae, foraminifers and echinoids) and terrigenous detritus (quartz and feldspars), bounded by magnesium-calcite or aragonite and, to a lesser extent, quartz cement (El Sayed 1988).

#### Wave characteristics, longshore currents and littoral drift rates

Wave action along the Mediterranean coast of Egypt is highly seasonal in intensity and direction, being strongly related to large-scale pressure systems over the Mediterranean and the North Atlantic (Hamed 1983; Nafaa et al. 1991). Accordingly, the wave climate may be subdivided into three seasons. Winter extends from November to March, spring from April to May, and summer from June to October. Wave data collected over a composite 10-month period at El Hamra pier were analyzed for this study. A wave rose diagram for the 10-month period of wave refraction analysis is depicted in Fig. 6A. The data exhibit low-amplitude swell during the spring and summer, with wave heights rarely exceeding 1–1.5 m. The wave direction is predominantly from the WNW and rarely from the NE. Winter waves are much higher than summer waves, fluctuating between stormy and fair-weather intervals and approaching from the N, NNW and NW sectors. These are the waves we would expect to contribute most to morphological change.

The relationship between wave climate and the present shoreline orientation ( $40^\circ$  to the north) shows effective oblique wave exposures (Fig. 6A). According to the relationship between the effective angle of incident waves and average shoreline orientation, two main wave exposure components are responsible for generating NE and SW sediment transport (see the two arcs in Fig. 6A). In general, the predominant wave components propagating from the NNW, N, NNE, NE, ENE and E are responsible for the generation of longshore currents toward the southwest, in total adding up to 90.2%. Waves from the NW, WNW and W sectors, on the other hand, generate a reverse longshore current toward the northeast, particularly during March and April, in total contributing a mere 5.7% (Fig. 6A). The remaining component (4.1%) represents calm conditions associated with winds blowing from the south and southeast. Perpendicular wave approach parallel to the line normal to the present coastline orientation represents an angle of incident waves close to zero, i.e., net zero transport. On the whole, the average significant wave height and

**Fig. 6A, B** The Alexandria coastline showing **A** the wave climate (wave rose along with the average orientation of the present-day coastline and the two main wave exposures inducing northeasterly and southwesterly sediment transport, indicated by *arches*), and **B** percentages of longshore current direction and littoral transport rate (littoral drift)



period are 0.7 m and 7.0 s, respectively. Generally, the average wave direction-height frequency distribution reveals that wave heights between 0.5 and 1.0 m dominate over those with heights of  $> 1-2$  m. The wave data show that low-swell waves prevail during spring and summer, wave heights rarely exceeding 1.2 m.

The N, NNW and NW waves are important in inducing morphological changes because of their long duration, particularly in winter. They are responsible for the net longshore sediment transport generated along the Alexandria coast. NNE and NE components occasionally also occur during April and May. The results obtained from the graphical analysis of waves against shoreline orientation are confirmed by the longshore currents measured at nine sites along the coastline. During the entire period, the measured longshore currents show that the predominant current direction was to the southwest (average = 38; range 16–54%), with a maximum current speed of  $143 \text{ cm s}^{-1}$  (Fig. 6B). Conversely, northeast-directed longshore currents (average = 26; range 11–43%) reached a maximum speed of  $96 \text{ cm s}^{-1}$ . Cross-shore currents were also recorded,

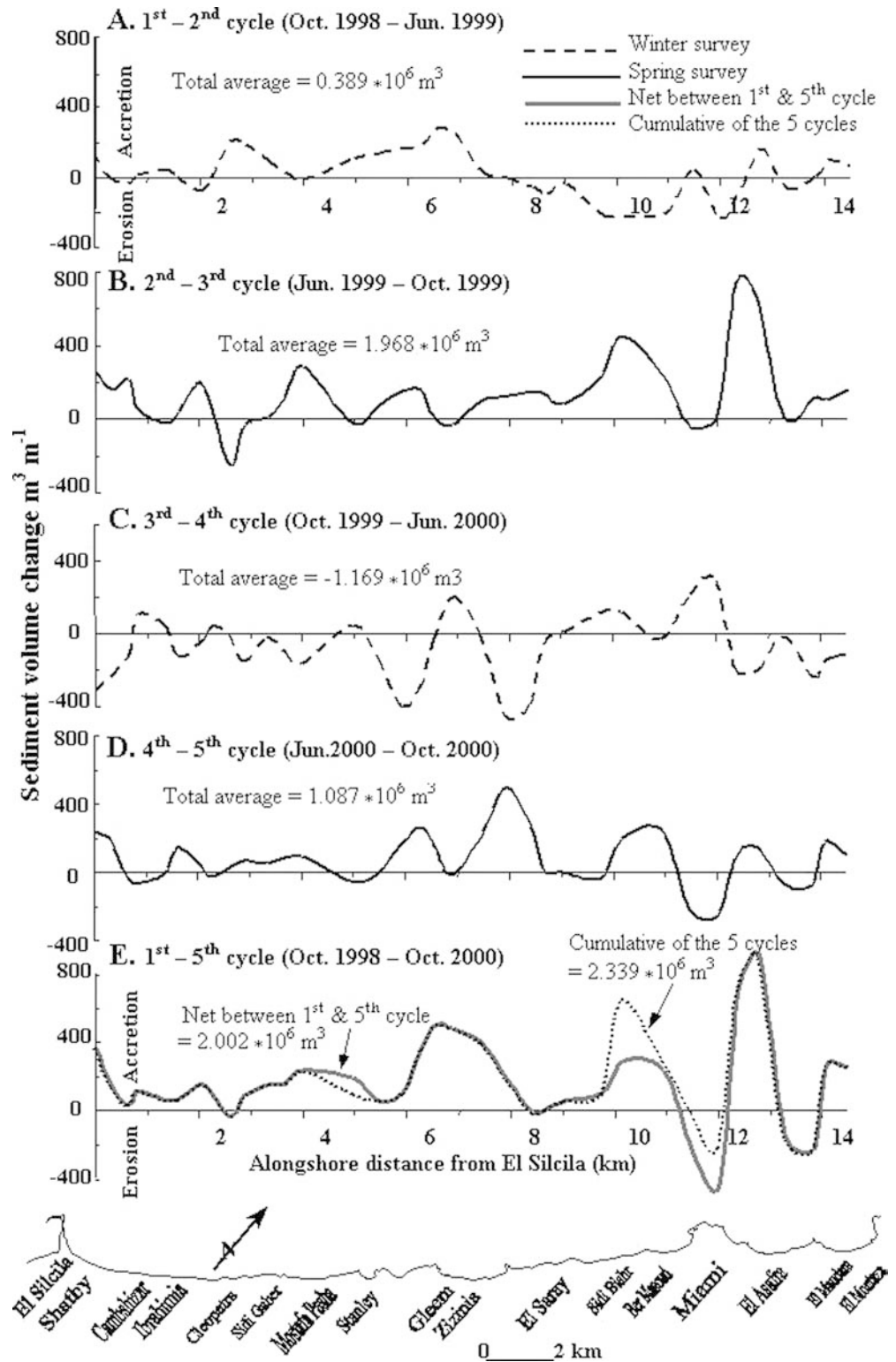
including onshore currents (6–24%, averaging 12%) and offshore rip currents (0.4–2.5%, averaging 1%).

Annual drift rates in the surf zone measured by fluorescent sand tracers at six stations reveal small values of  $< 0.26 \times 10^6 \text{ m}^3$  as compared to the Nile delta where they range between  $1.8$  and  $3.2 \times 10^6 \text{ m}^3 \text{ year}^{-1}$  (Badr and Lotfy 1999). The percentage occurrence of littoral drift varies in intensity and direction from site to site, due to the changing morphology of the coastline and resulting changes in wave exposure. The percentage occurrences of littoral drift components heading southwest, northeast, offshore and onshore correspond to littoral drift rates of 0.0–0.21, 0.0–0.17, 0.23–0.34 and  $0.12-0.17 \times 10^6 \text{ m}^3 \text{ year}^{-1}$ , respectively (Fig. 6B). These low littoral drift rates are attributed to the morphological nature of the coastline versus wave directions.

#### Longshore volumetric change

In this study, the autumn (September/October) and spring (April/May) survey periods were used to determine

**Fig. 7A–E** Seasonal variability of net volumetric changes of sediment alongshore of the Alexandria coast. The pattern indicates that the littoral zone of Alexandria is gaining sediment in summer and losing sediment in winter, and also reflects the influence of bedrock irregularity



seasonal changes in sediment volume (Fig. 7). Spring profiles record changes due to storm waves prevailing during the preceding winter season, whereas autumn profiles yield changes induced from swell waves occurring during the spring/summer seasons. The winter season extends from November to March, and is the period of

most intense coastal erosion (Elwany et al. 1988). On average, 16 winter storms occur, seven of which are associated with heavy rain and severe winds. In this study, the alongshore changes in sediment volume for the 37 beach profiles were determined between the five successive survey cycles (autumn and spring surveys). There-

fore, the sediment volumes between successive survey cycles, i.e., between the 1st and 2nd, the 2nd and 3rd, the 3rd and 4th, and the 4th and 5th cycles, yield data on winter followed by spring/summer conditions over the study period, with intervals ranging in duration from 5 to 7 months. The total profile change over the entire study period has also been assessed.

Net volumetric changes of sediment per meter ( $\text{m}^3 \text{m}^{-1}$ ) were determined for all available beach-nearshore profile data along the entire length of the study area. Figure 7 shows the distribution of sediment volumes ( $\text{m}^3 \text{m}^{-1}$ ) up to 10-m water depth (maximum of  $\sim 1$  km offshore distance) along the 14.5 km of monitored shoreline. Calculations were performed for each of the profile lines between successive surveys (autumn and spring surveys). The volume changes fluctuate in the range  $-400$  to  $+800 \text{ m}^3 \text{m}^{-1}$ , with a significant longshore trend over the study period. The variations in sediment volume during individual erosion/accretion/erosion cycles (Fig. 7) show a series of "saw-tooth" peaks, the largest changes corresponding to areas of sandy seabed, decreasing alongshore toward areas composed of bedrock.

---

## Discussion

### Seafloor morphology

The morphology of beaches can be characterized as ranging from dissipative to reflective (Wright and Short 1983, 1984), depending on the grain size, beach slope, and wave parameters. The gently to steeply sloping surf zones within the Alexandria littoral cell can easily be distinguished in the classification scheme, wherein the beaches range from dissipative to reflective. Compared with the Nile delta, Alexandria beaches have been designated as refractive due to the steeply sloping, coarse-grained nearshore zone (Nafaa and Frihy 1993). The results obtained from the profile and sediment analyses in the study area indicate that the beaches associated with gently sloping nearshore zones, as those of sub-area II (1:40), are moderately dissipative (Fig. 4B, C). These beaches cause the waves to break across a wide surf zone, thereby dissipating most of their energy. The beaches fronted by steeply sloping surf zones, by contrast, tend to be reflective, their steeper slopes allowing the incident waves to break closer to the shore. This is the situation in sub-area I (1:10). Both the reflective and dissipative beaches are mostly composed of fine-grained sediment (0.15–0.45 mm) derived from artificial sand nourishment and fluvial contribution (Fig. 5A). The bedrock outcrops, islets and other submerged features on the seabed serve to dissipate wave energy within the surf zone, thereby modifying the predominant sediment transport direction to the NE or to the SW. This would be expected from bedrock alignment influencing current action within the littoral cell.

The elevated nearshore zone is a remnant of carbonate ridge #0 which has been identified by Butzer (1960), whereas the offshore part represents the seaward trough of that ridge.

### Sedimentary facies and seafloor provinces

The fine- and coarse-grained sediment groups of beach and seabed sediments outlined in Fig. 5 represent a classical mixing pattern of two discrete sediment populations, as postulated by Folk and Ward (1957), Folk and Robles (1964) and Flemming (1988). However, local differences between these sediment groups can be accounted for by both mixing between two independent source populations as well as progressive sorting.

This textural difference is also reflected in the composition of the sand-sized fraction of the two sediment groups. The petrologic and faunal characteristics of the coarse-grained sediments are very similar to those identified as relict and reworked relict (palimpsest) sands recovered off the Nile delta between the coast and the continental shelf break (Summerhayes et al. 1978; Stanley and Bernasconi 1998). Equivalent nearshore and coastal relict sediments have accumulated over many continental shelves worldwide, mostly in the course of the Flandrian transgression (Emery 1968; Swift et al. 1971; Wilson 1988). Off the Nile delta, relict sediments of fluvial origin began to accumulate shortly after the maximum eustatic sea-level lowstand when the coastline had advanced northward to the outer edge of the continental shelf (Stanley and Bernasconi 1998). Such relict sediments contain infralittoral molluscan faunas usually living at depths of  $< 25$  m, and considered as relict markers of former low sea-level stands of late Pleistocene to mid-Holocene age ( $\sim 16,000$ – $9,000$  years B.P.). Where concentrated, such shallow-water faunas and associated sediments record effects of seafloor erosion by current activity which prevailed over the shelf since it was drowned by the rising sea level in late Pleistocene to mid-Holocene times (Stanley and Bernasconi 1998). In this study, relict faunas identified in the coarse-grained sediments (cf. the first 10 species listed above) resemble those of infralittoral molluscan faunas previously identified by Stanley and Bernasconi (1998) in surficial sediments off the Nile delta. In the same samples, shallow-water bryozoans (Abdel-Aal and Frihy 1987) and foraminifers (Abdou et al. 1991) were also recorded. Based on petrologic and faunal composition, the examined sediment samples can be assigned to a recent fine-grained and a relict coarse-grained sand facies. A comparison between the petrologic components of these two facies is shown in Fig. 4A. The recent fine-grained sand facies is composed of a variable mixture of carbonate grains (43%) and light minerals (44%), in which the proportion of carbonate increases westward (Fig. 4F). The presence of light (quartz and feldspar) and heavy minerals (particularly in the east) indicates fluvial input from the Nile delta region. Deltaic

sediments occasionally drifting westward due to current reversals induced by waves propagating from the NE and E have been reported by Fanos et al. (1991). This explains that sediments enter the littoral cell system by bypassing the Abu Quir headland during seasonal reversals in current direction. Part of these bypassed sediments may be related to the former Canopic branch of the Nile delta which discharged onto the shallow shelf in the westernmost part of Abu Quir Bay during the late Holocene (Fig. 1A). This distinct branch was first explored in this sector by Toussoun (1934).

The relict coarse-grained sand facies is predominantly composed of carbonate grains (73%) largely consisting of shells (15%). The lower proportion of heavy minerals (0.9%) and the deficiency of light grains (12%) suggest that they were originally eroded from a carbonate ridge (Fig. 4A). The high proportion of poorly preserved fossils and shell fragments (15%) indicates strong sediment reworking and long transport distances during the Holocene transgression. We contend that the occurrence of this relict sand facies on the shallow inner shelf of Alexandria may have resulted from landward and lateral displacement (i.e., palimpsest) from their original position on the middle and outer shelf. Their widespread distribution along the lower part of the nearshore zone (8–10 m) records the effects of progressive net landward displacement through time by off/onshore transport by storm waves and bottom currents. In the case of a high-relief seabed, the ridge trough acts to confine the relict sediment to places where it is subjected to downslope (offshore) gravity transport (Fig. 4B). Rather, shore-parallel linear distributions are primarily a response to prevailing northeasterly-directed currents and the southwesterly current reversals since the early Holocene.

The modern shoreline was thus created by a slowly rising sea level crossing this carbonate surface during the Holocene marine transgression. Coarse-grained sands covering the rocky seafloor formed during this transgression by initial erosion of this surface (Fig. 4B). Differences in bedrock lithology influenced the erosional characteristics which, in turn, controlled the morphology of the present nearshore area. As sea level continued to rise, these sands were subsequently reworked and deposited in depressions on the seafloor by Holocene to modern currents and biogenic activity (cf. Stanley and Bernasconi 1998). It is generally accepted that world sea level rose from ~120 m below present to its present-day position during the past 18,000 years (Fairbanks 1989). With the melting of glaciers and thermal expansion of seawater, there was initially a rapid rise in sea level, averaging about 8 mm year<sup>-1</sup>, until approximately 7,000 years B.P. when it slowed to 1–2 mm year<sup>-1</sup> (the present-day eustatic sea level).

The distribution of the recent fine-grained sand facies across the study area tends to biolastic carbonates in the west and terrigenous material in the east (Fig. 4F). Their distributions reflect the coast-parallel northeastward transport by littoral currents. They are reworked and displaced by alongshore and cross-shore transport

processes leading to the formation of pocket beaches and embayed sandy beaches, as well as sand blankets on the low-lying surfaces of the irregular rocky seabed, mostly between elevated rock outcrops. The undulating coastline and the irregular bedrock morphology have induced a different set of nearshore processes. These processes have influenced the spatial patterns in seabed grain size and carbonate contents. The alongshore and cross-shore increase and decrease in rhythmic patterns observed in these sand facies and their associated carbonate contents are largely a response to sedimentary sources, progressive sorting, and dispersal toward the northeast and in a cross-shore direction.

Accordingly, there are two major sources contributing to the sediment of the littoral cell of Alexandria. The principal source is the eroded older “Pleistocene” seabed limestone ridges which supply large amounts of carbonate grains formed during the Holocene transgression. They mostly consist of well-sorted coarse sand rich in fossils and shell fragments. The second source, which is influenced by late Holocene and modern oceanographic processes, and contributes moderately sorted fine sand consisting of variable mixtures of quartz and carbonate grains, is supplied from the desert in the course of beach nourishment projects and as filling material used in widening the coastal Corniche. The relict, coarse-grained sands are also contributed in appreciable amounts from the modern sand blanketing the nearshore area. Visual examination of the size-frequency curves has indicated that the sediments of both groups are well sorted and essentially unimodal, although a few samples of the fine-grained sediment group are slightly bimodal. This confirms that over time the source materials contributed to the littoral cell, both from beach nourishment and deltaic origin, have reached a state of compatibility in their grain-size distributions. Previous studies have assumed that the sediment grain size of the littoral zone reverts gradually to the original distribution after a certain period of time following beach nourishment (e.g., Krumbein and James 1965).

One of the critical parameters in designing protective structures is defining the depth, and hence distance, offshore of active sediment movement by waves, i.e., the depth of closure. Previous studies have used distinct changes in sediment characteristics (color, texture, heavy minerals and benthic faunas) along shore-normal profile as geological indicators to delineate depth of closure, i.e., the seaward depth limits at which significant wave energy levels interact with a sand bed (Hallermeier 1981). The long-term exposure of the relict coarse-grained sand facies indicates that they are not influenced by the nearshore fine-grained sediment dispersed by seaward-directed currents. However, abrupt changes in the sediment grading between the recent fine- and the relict coarse-grained sand facies indicate the transition between highly active and inactive zones, respectively. In addition to texture, the mineralogical and faunal composition of the sand-sized fraction as well as the relative

percentages of stained grains suggest insignificant cross-shore exchange between the two facies (Fig. 4A, D). Therefore, the offshore boundary between the recent and relict sand facies can be used to define the depth of closure of the littoral cell of Alexandria. Accordingly, this boundary is positioned between 8- and 10-m water depth. Beyond this depth, there is no significant net sediment transport. Owing to the strong variability in the seabed slope of the nearshore zone, the 8–10 m depth contour is located between 400 and 800 m offshore (Fig. 4D). These limits are almost identical to those derived from beach profile analyses at Alexandria by Iskander (2000).

### Coastal processes

The Alexandria coast is characterized by high wave energies particularly in winter. Based on the results of this study, waves induce opposing SW and NE longshore currents. The higher proportion of SW currents is attributed to the large angle between the incident waves and the average shoreline orientation and geometry, as well as to the irregularity of the seabed and the undulating coastline. This situation differs from that recorded at the Nile delta and indicates that southwesterly littoral currents at Alexandria are strong enough to transport sediment along the coast. By contrast, easterly littoral currents are more dominant along most of the Nile delta coastline, with only occasional reversals to the west (Fanos et al. 1991).

The major headlands occurring along the shore of Alexandria extend into the surf zone and confine the beach sands to littoral-cell embayments and pocket beaches, with little or no bypassing. This, in effect, makes the Alexandria resort cell area an extended pocket beach and implies that the long-term net littoral drift is close to zero. Direct evidence for this zero net littoral drift has come from field observations of sand accumulation patterns adjacent to the groins constructed along the Alexandria coast, where sand is being deposited both to the immediate east and west of the groins. The seasonal reversal in the direction of sand transport along the beach is predominantly northeast during the winter and summer months, and southwest during autumn and spring, but with a zero net littoral drift when averaged over several years.

### Volumetric changes of sediments

The traditional way to analyze morphodynamic changes induced by marine processes is to assess the temporal and spatial changes of sediment volumes from beach profile data. Storms tend to move sand rapidly offshore whereas, under lower-energy conditions, sand moves onshore, causing gradual beach accretion (Komar 1976). This cyclicity is reflected in profile changes along the littoral cell of Alexandria, being induced by seasonal

changes in wave climate. Such cyclicities have been documented along many sandy beaches worldwide (Shepard 1950; Winant et al. 1975; Stive et al. 1990).

In terms of seasonality, the overall net change was erosional for the winter period, except for the accretionary period between the 1st and 2nd surveys when a small net gain of  $0.389 \times 10^6 \text{ m}^3$  was recorded (Figs. 7 and 8). The winter pattern reversed to accretion over the next spring period between the 2nd and 3rd surveys, with  $1.968 \times 10^6 \text{ m}^3$  accumulation. The remaining periods show a similar trend, with a sediment loss in winter followed by a sediment gain in spring. Of particular importance is the average sediment volume calculated between the 1st and 5th cycles ( $2.002 \times 10^6 \text{ m}^3$ ), as it approximates the total average volume calculated for the whole period ( $2.339 \times 10^6 \text{ m}^3$ ). This similarity is consistent with the close parallelism of the alongshore total volume change curves (Fig. 7E). This indicates that the amount of sediment within the littoral cell of Alexandria remained nearly constant during the study period. The compartment nature of the bedrock, together with the two main headlands at El Silcila and El Montaza supported by the closure depth (8–10 m) thus trap sediment within the littoral cell.

The alongshore variations in sediment volume over the study cycles (Fig. 7) show an undulating trend, the largest changes corresponding to areas of sandy seabed, decreasing alongshore toward areas composed of bedrock. This pattern can be attributed to the rough, irregular rocky seabed associated with a deficiency of sediment. Generally, changes in sediment volume systematically increase toward the east, with a maximum change of  $800 \text{ m}^3 \text{ m}^{-1}$  along the eastern embayment of El Asafra. This large embayment has been subjected to artificial beach nourishment operations (Frihy and Dean 1992; Iskander 2000).

An attempt was made to evaluate the budget of the littoral zone of Alexandria to determine if sediment is being lost or gained over time. The total average sediment volume for the entire study area was assessed using linear regression analysis to calculate the temporal variations of sediment volume for each successive survey

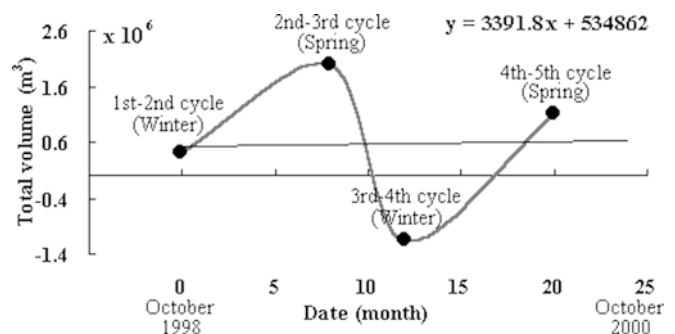


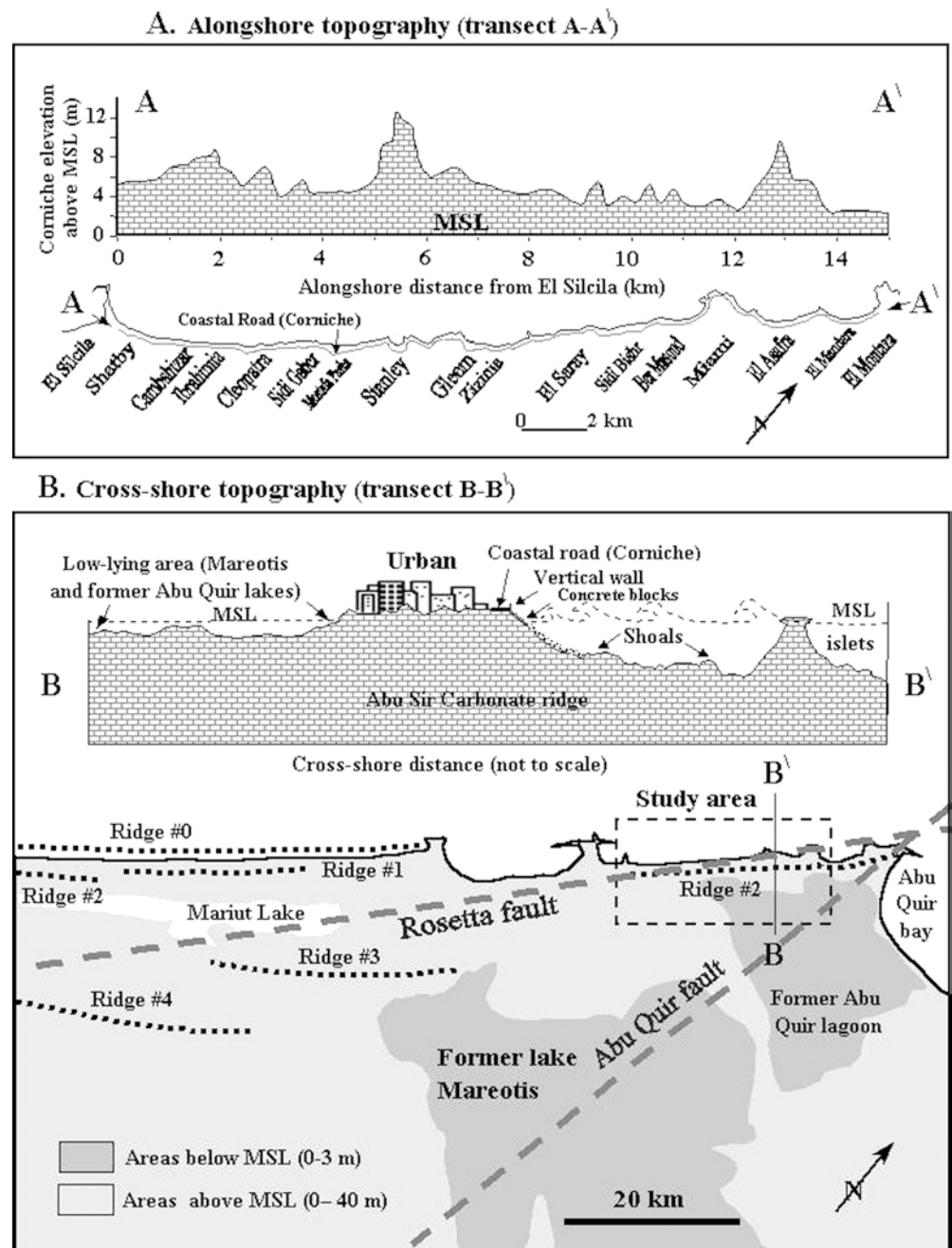
**Fig. 8** Time series of average net volumetric changes of sediment for the survey intervals between the examined profile survey cycles, illustrating that there is a slight annual gain in sediment amounting to  $0.041 \times 10^6 \text{ m}^3 \text{ year}^{-1}$ . This gain may be due to engineering works to widen the coastal road, and to illegal dumping of sediment

interval (Fig. 8). The slightly rising mean trend line indicates that the study area is gaining small amounts of sediment at a rate of  $0.041 \cdot 10^6 \text{ m}^3 \text{ year}^{-1}$ . An interesting question is why the littoral cell is gaining sediment over time. Our interpretation is that an additional source of sediment may be the large engineering works which were undertaken to widen the coastal Corniche (Figs. 2E and 3). Excess detrital sediments comprising sand and gravel (granules, pebbles, cobbles and large boulders) armored by concrete blocks have been dumped in the area (Fig. 3). The volume of excess sediment amounts to ca.  $1.1 \cdot 10^6 \text{ m}^3$  and was dumped periodically in the course of the five phases of the project, in proportions of 1, 6, 24, 32 and 37%, respectively.

## Relative sea-level rise and backshore elevation

In this study, the elevation of the coastal Corniche backing the beach has been surveyed to assess the degree of vulnerability to relative sea-level rise. Previous tide gauge analyses indicate that relative sea-level rise in the vicinity of Alexandria ranges from 2 to 2.9  $\text{mm year}^{-1}$  (El Fishawi and Fanos 1989; El Din et al. 1989; Frihy 1992). Emery et al. (1988), by contrast, reported an uplift rate of  $-0.7 \text{ mm year}^{-1}$  using a short time series of annual tide gauge records. These rates differ from those observed further to the east in the Nile delta, which exhibits a high relative sea-level rise of the order of 2.2  $\text{mm year}^{-1}$  (El Fishawi and Fanos 1989) to 4  $\text{mm year}^{-1}$  (Emery et al.

**Fig. 9A** Alongshore elevation of the coastal road Corniche backing the Alexandria coastline (transect A-A').  
**B** Schematic cross-shore profile showing the general backshore topography (transect B-B'). General topography of Alexandria showing the location of the carbonate ridges crossing the Alexandria region (modified after Warne and Stanley 1993). The Rosetta and Abu Quir faults are positioned after Zaghoul and Elgamal (1999)



1988). Updated time series data recorded at Alexandria's western harbors (1944–2000; 54 years) have been published by Frihy (2003). His results indicate that the mean sea level at Alexandria has risen  $1.6 \text{ mm year}^{-1}$  between 1944 and 2000. Land subsidence along the Alexandria coast is complicated by the local tectonic setting. Previous studies have indicated small values of both land emergence and subsidence ranging from  $-0.5$  to  $2.2 \text{ mm year}^{-1}$  (Chen et al. 1992; Warne and Stanley 1993). Warne and Stanley (1993) attributed this land uplift to neotectonic uplift along two major faults crossing the Alexandria region, the Rosetta and Abu Quir faults (Zaghloul and Elgamal 1999; Fig. 9).

Although previous studies have indicated that the coastline of Alexandria and the Nile delta are vulnerable to a rising sea level resulting from expected climate changes (Broadus et al. 1986; Milliman et al. 1989; El Sayed 1991; Delft Hydraulics and CRI 1991; Sestini 1992; El Raey et al. 1995), these studies have not considered the backshore topography of Alexandria in their assessments. In this study, the elevation of the coastal Corniche backing the beach has been measured to assess the degree of vulnerability to relative sea-level rise. The Alexandria beaches have an elevation between zero and 2 m above mean sea level. These are backed by the Corniche which is relatively high in elevation, with a marked alongshore variability ranging between 2.41 and 12.27 m relative to mean sea level (Fig. 9A). The highest elevation exists at Stanley and in the Miami-Asafra area, the lowest at El Mandara. The substantial undulation of the Corniche surface reflects the original topography of the carbonate ridges running parallel to the coastline and which form the coastal plain of Alexandria (Fig. 9A, B). Generally, the elevated land forming the back-beach of Alexandria acts as a natural defense barrier against beach erosion, and possibly against consequences of SLR. In terms of surface topography, the backshore of Alexandria ranges in elevation between zero and 40 m, some parts even lying below sea level (0–3 m; Fig. 9B), for example, the present-day Mariut lake, the former Abu Quir and Mareotis lagoons, and the cultivated land bordering the southern margins of Alexandria. These low-lying areas are vulnerable to flooding under extreme run-up events during storm surges. Since the barrier fronts the low-lying land south of the city (Fig. 9B), not all of the coastal plain of Alexandria will be vulnerable to the impacts of future SLR.

## Conclusions

The littoral cell of Alexandria is unusual in that it is longshore transport-dominated, has a small sand budget, and receives little sand from freshly weathered rock, artificial nourished sand, and palimpsest offshore sediment. These sediments show a seasonal cyclicity induced by changes of wave climate.

The irregular bedrock of the Alexandria littoral cell is blanketed by two sand facies exhibiting proportional

mixing of carbonate-siliciclastic sands, controlled by sediment sources, morphologic features, hydrodynamic processes and sea-level rise. They are moving as bedload carpet on the bedrock surface in opposing directions toward the NE and SW under the action of wave-induced longshore currents.

The bedrock system fronting the coastline of Alexandria allows wave dissipation and can be involved in artificial protection works. The pronounced raised features on the sea bottom can be considered as a toe for hard protective structures or for sand nourishment. Nourishment is an environmentally friendly measure to mitigate storm-induced-beach erosion and flooding, particularly for the lowest elevation points ( $<3 \text{ m}$  high), as well as enhancing the aesthetic view of the waterfront of the city. The coarse-grained sediments existing offshore can be used as a source of "borrow" material for beach nourishment. Further investigations are needed to provide insight into the compatibility, geographical dimensions and sediment volume of this source.

**Acknowledgements** This study was undertaken as part of the Coastal Research Institute program to monitor morphodynamic changes along the Alexandria coast. The authors appreciate the assistance and efforts the staff of the Coastal Research Institute contributed in the field and laboratory activities of this study. We also express our appreciation to Dr. Deborah Lawrence, University of Reading, UK, whose review helped to improve this manuscript. Also appreciated is the help of Dr. Mahmoud Kh. El Sayed, Oceanography Department, Alexandria University of Egypt, and Dr. A. Abdel-Aal, Geology Department, for identification of the molluscan faunas.

## References

- Abdel-Aal AA, Frihy OE (1987) Study of Bryozoa in the sediments of the Nile delta continental shelf. *Bull Inst Oceanogr Fish Egypt* 13:269–280
- Abdou HF, Samir AM, Frihy OE (1991) Distribution of benthonic foraminifera on the continental shelf off the Nile delta. *N Jahrb Geol Paläontol Mn Stuttgart* 1:1–11
- Badr AA, Lotfy MF (1999) Tracing beach sand movement using fluorescent quartz along the Nile Delta promontories, Egypt. *J Coastal Res* 14:261–265
- Broadus JJ, Milliman S, Edwards D, Aubrey, Gable F (1986) Rising sea level and damming of rivers: possible effects in Egypt and Bangladesh. In: Titus J (ed) *Effect of changes in stratospheric ozone and global climate*, Paris, vol 4, pp 165–189
- Butzer KW (1960) On the Pleistocene shorelines of Arabs' Gulf, Egypt. *J Geol* 68:626–637
- Chen Z, Warne AG, Stanley DJ (1992) Late Quaternary evolution of the northwest Nile delta between Rosetta and Alexandria, Egypt. *J Coastal Res* 8:527–561
- Delft Hydraulics, CRI (1991) Implication of relative sea-level rise on the development of the lower Nile delta, Egypt. Pilot study for a quantitative approach, final report. Delft Hydraulics, CRI
- El Din SH, Khafagy AM, Fanos AM, Ibrahim AM (1989) Extreme sea level values on the Egyptian Mediterranean coast for the next 50 years. *Int Sem Climatic Fluctuations and Water Management*. Water Research Centre, Cairo
- El Fishawi NM, Fanos AM (1989) Prediction of sea level rise by 2100, Nile delta coast. INQUA, Commission Quat Shorelines *Newslett* 11:43–47



- El Raey M, Nasr S, Frihy O, Desouk S, Dowidar Kh (1995) Potential impacts of accelerated sea-level rise on Alexandria, Governorate, Egypt. *J Coastal Res* 51:190–204
- El Sayed MKh (1987) Progressive cementation in Pleistocene carbonate sediments along the coastal area of Alexandria. *J Coastal Res* 4:163–172
- El Sayed MKh (1988) Sea level rise in Alexandria during the late Holocene: archaeological evidences. *Rapp Comm Int Mer Méditerranée*
- El Sayed MKh (1991) Implications of climatic changes for coastal areas along the Nile Delta. *Environ Prof USA* 13:59–65
- El Wakeel SK, El Sayed MKh (1978) The texture, mineralogy and chemistry of bottom sediments and beach sands from Alexandria region. *J Mar Geol* 27:137–160
- El Wakeel SK, El Sayed MKh, Mahmoud B (1980) The evolution of Alexandria beaches: a preliminary study. *Thalassia Jugoslavica* 16:1–8
- Elwany MH, Khafagy AA, Inman DL, Fanos AM (1988) Analysis of waves from arrays at Abu Quir and Ras El Bar, Egypt. *Advances in Underwater Technology: Ocean Science and Off-shore Engineering*, vol 16, pp 89–97
- Emery KO (1968) Relict sediments on continental shelves of worlds. *AAPG Bull* 52:445–464
- Emery KO, Aubrey DG, Goldsmith V (1988) Coastal neo-tectonics of the Mediterranean from tide-gauge records. *J Mar Geol* 81:41–52
- Fairbanks RG (1989) A 17,000 year glacio-eustatic sea level record: influence of glacial melting on the younger Dryas event and deep-ocean circulation. *Nature* 342:637–642
- Fanos AM, Frihy OE, Khafagy AA, Komar PD (1991) Processes of shoreline change along the Nile Delta coast of Egypt. *Coastal Sediments'91 Conf USA*, vol 2, pp 1547–1557
- Flemming BW (1988) Process and pattern of sediment mixing in a microtidal coastal lagoon along the west coast of South Africa. In: de Boer PL, van Gelder A, Nio SD (eds) *Tide-influenced sedimentary environments and facies*. D Reidel, Dordrecht, pp 257–288
- Folk RL, Robles R (1964) Carbonate sediments of Isla Perez, Alacran Reef Complex, Yucatan. *J Geol* 72:255–292
- Folk RL, Ward WC (1957) Brazos river bar: a study in the significance of grain size parameters. *J Sediment Petrol* 27:3–27
- Fourtau R (1893) La région de Maryut; étude géologique. *Bull Inst Egypt Sér* 3:1–141
- Frihy OE (1992) Sea level rise and shoreline retreat of the Nile delta promontories, Egypt. *Natural Hazards Netherlands* 5:65–81
- Frihy OE (2003) The Nile delta-Alexandria coast: vulnerability to sea-level rise, consequences and adaptation. *Mitigation Adaptation Strategies Global Changes* 8:115–138
- Frihy OE, Dean R (1992) Artificial beach nourishment projects on the Egyptian coast. In: *Int Coastal Congr ICC Kiel'92*, 7–12 September 1992, pp 84–95
- Frihy OE, Stanley DJ (1988) Texture and coarse fraction composition of Nile delta deposits: facies analysis and stratigraphic correlation. *J Afr Earth Sci* 7:237–255
- Hallermeier RJ (1981) A profile zonation for seasonal sand beaches from wave climate. *Coastal Eng* 4:253–277
- Hamed AA (1983) Atmospheric circulation features over the southeastern part of the Mediterranean Sea in relation to weather conditions and wind waves along the Egyptian coast. PhD Thesis, Faculty of Science, Alexandria University
- Hamed AA, El Gindy AA (1988) Storm surge generation by winter cyclone at Alexandria, Egypt. *J Int Hydrogr Rev Monaco* 36:129–139
- Hilmy ME (1951) Beach sands of the Mediterranean coast of Egypt. *J Sediment Petrol* 21:109–120
- Ingle JC Jr (1966) *The movement of beach sand*. Elsevier, New York, *Developments in Sedimentology Series* 5
- Iskander MM (2000) Sediment transport along Alexandria coast. MSc Thesis, Faculty of Engineering, Alexandria University
- Iskander MM, El-Ansary AE, Abd El-Mooty MM, Nagy HM (2004) Modified N-line numerical model for mapping bottom topography changes—case study Edko city, Egypt. *J Faculty of Engineering, Alexandria University* (in press)
- Komar PD (1976) *Beach processes and sedimentation*. Prentice-Hall, Englewood Cliffs, NJ
- Krumbein WC (1963) Application of logarithmic moments to size frequency distributions of sediments. *J Sediment Petrol* 6:35–47
- Krumbein WC, James WR (1965) A lognormal size distribution model for estimating stability of beach fill material. Coastal Engineering Research Center, US Army Eng Waterw Exp Station, Vicksburg, MS, Rep TM-16
- Lindell LT, Alexandersson ET, Norman JO (1991) Satellite mapping of oolitic ridges in Arabs Gulf, Egypt. *J Geocarto Int Sweden* 1:49–60
- Milliman JD, Broadus JM, Gable F (1989) Environmental and economic implications of rising sea level and subsidence deltas: the Nile and Bengal examples. *Ambio* 18:340–345
- Nafaa MG, Frihy OE (1993) Beach and nearshore features along the dissipative coastline of the Nile delta, Egypt. *J Coastal Res* 9:423–433
- Nafaa MG, Fanos AM, El Ganainy MA (1991) Characteristics of waves off the Mediterranean coast of Egypt. *J Coastal Res* 30:25–34
- Perlin M, Dean RG (1983) A numerical model to simulate sediment transport in the vicinity of coastal structures. US Army Corps of Engineers, CERC, Fort Belvoir, Misc Rep 83-10
- Said R, Philip G, Shukri NM (1956) Post Tyrrhenian climatic fluctuations in northern Egypt. *Quaternaria* 3:167–172
- Sestini G (1992) Implications of climate change for the Nile delta. In: Jetic L, Milliman JD, Sestini G (eds) *Climate change and the Mediterranean*. Environmental and societal impacts of climate and sea-level rise in the Mediterranean Sea. Edward Arnold, London, pp 533–601
- Shepard FP (1950) Longshore bars and longshore troughs. Beach Erosion Board, US Army Corp of Engineers, Washington, DC, Tech Memo 15
- Shukri NM, Philip G, Said R (1956) The geology of the Mediterranean coast between Rosetta and Bardia. Part II. Pleistocene sediments: geomorphology and microfacies. *Bull Inst Egypt* 37:395–427
- Silvester RJ, John RC (1993) *Coastal stabilization*. Prentice-Hall, Englewood Cliffs, NJ
- Stanley DJ, Bernasconi MP (1998) Relict and palimpsest depositional patterns on the Nile shelf recorded by molluscan faunas. *Palaios* 13:79–86
- Stive MJ, Roelvink DA, De Vriend JJ (1990) Longterm scale coastal evolution concept. In: *Proc 22nd Coastal Engineering Conf ASCE*, New York, pp 1962–1974
- Summerhayes CP, Sestini G, Misdorp R, Marks N (1978) Nile delta: nature and evolution of continental shelf sediments. *Mar Geol* 27:43–65
- Swift DJ, Stanley DJ, Curray JR (1971) Relict sediment on continental shelves: a reconsideration. *J Geol* 79:322–346
- Toussoun O (1934) Les ruines sous-marines de la Baie d'Abukir. *Bull Soc R Archéol Alexandria* 29:342–352
- Warne AG, Stanley DG (1993) Late Quaternary evolution of the northwest Nile delta and adjacent coast in the Alexandria region, Egypt. *J Coastal Res* 1:26–64
- Wilson JB (1988) A model of temporal changes in the faunal composition of shell gravels during a transgression on the continental shelf around the British Isles. *Sediment Geol* 60:95–105
- Winant CD, Inman DL, Nordstorm CE (1975) Description of seasonal beach changes using empirical eigen functions. *J Geophys Res* 80:1979–1986
- Wright LD, Short AD (1983) Morphodynamics of beaches and surfzones in Australia. In: Komar PD (ed) *CRC handbook of coastal processes and erosion*. CRC Press, Boca Raton, FL, pp 35–64
- Wright LD, Short AD (1984) Morphodynamic variability of surfzone and beaches: a synthesis. *Mar Geol* 56:93–118
- Zaghloul ZA, Elgamel MM (1999) Deltas modern and ancient. In: Zaghloul ZM, Elgamel MM (eds) *Deltas—modern and ancient*. Proc 1st Int Symp Deltas, Mansoura University, Egypt